# Numerical modeling of initial slip and poroelastic effects of the 2012 Costa Rica earthquake

McCormack, Kimberly A.[1]*, Hesse, M. A.[1], Stadler, G.[2]
1.Department of Geosciences, The University of Texas at Austin *kimberly.mccormack@utexas.edu
2.Courant Institute of Mathematical Sciences, New York University

## Background

On September 5th, 2012 a major megathrust earthquake ($M_w$=7.6) ruptured the plate interface beneath the Nicoya Peninsula, Costa Rica. The epicenter was located 12km offshore of the central Nicoya coast, at a depth of 18km. The rupture spread outward along the plate interface to encompass 3000 km$^2$ of the Nicoya seismogenic zone. More than 1,700 aftershocks were recorded within the first five days. With the exception of the imaged 'locked patch', the plate ruptured within a zone that previously deteremined to be seismically coupled.

The Nicoya Pennisula, uniquely positioned over the seismogenic zone the the subduction zone, allows more direct observations of fault slip via land-based GPS measurements. During the earthquake a total of 37 stations (both continuous and campaign) were deployed.

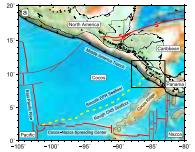


(Feng, 2012)

## Motivation

- **Is poroelastic relaxation a significant part of post-seismic deformation patterns?**
- **Can we differentiate it from afterslip and viscoelasticity?**
- **How is stress transferred by post-seismic fluid flow?**

## GPS Data / Model Outline

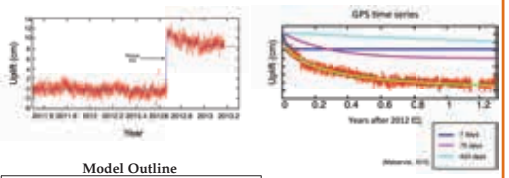


**Model Outline**

Surface displacement from GPS stations

Solve Inverse Problem

Instantaneous displacement on fault

Solve Forward Problem

Rock displacement and pore pressure evolution

We formulate a Bayesian inverse problem to infer the co-seismic slip on the fault plane based on instantaneous surface displacements taken from high-rate GPS stations (**top left**). The solution to the inversion is then taken as the initial condition to the time-dependent forward problem which models how both pore pressure and rock displacement evolve after the earthquake.

## Model Geometry

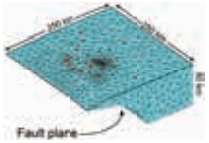


3D finite element model geometry (above). Red circles represent the locations of GPS stations.

**Elasticity Boundary Value Problem:**

$$\begin{aligned} -\nabla\cdot\boldsymbol{\sigma}(\mathbf{u}) &= 0 \quad \text{in } \Omega \\ \boldsymbol{\sigma}(\mathbf{u})\boldsymbol{n} &= 0 \quad \text{on } \Gamma_{top} \\ \boldsymbol{u} &= 0 \quad \text{on } \Gamma_{side} \\ \boldsymbol{u}\cdot\boldsymbol{n} &= 0 \quad \text{on } \Gamma_{bottom} \\ (\boldsymbol{I}-\boldsymbol{n}\boldsymbol{n}^\top)\boldsymbol{u} &= \boldsymbol{u_0} \quad \text{on } \Gamma_{bottom} \end{aligned}$$

## Inversion for slip distribution

To formulate the inverse problem, we assume a vector of surface observations $\boldsymbol{u}^{\text{obs}}$ and a corresponding surface observation operator $\mathcal{B}$, which evaluates the displacement at points on the top surface $\Gamma_{top}$. Then, the inverse problem with a regularization based on the distance between observation points for the unknown displacement $\boldsymbol{u_0}$ on $\Gamma_{bottom}$ is:

**Cost functional:**

$$\mathcal{J}(\boldsymbol{u_0},\boldsymbol{u}) = \min_{\boldsymbol{u_0}\in L^2(\Gamma_b)} \mathcal{J}(\boldsymbol{u_0}) := \frac{1}{2}(\mathcal{B}\boldsymbol{u}-\boldsymbol{u}^{\text{obs}})^\top \boldsymbol{\Gamma}_{\text{noise}}^{-1}(\mathcal{B}\boldsymbol{u}_d-\boldsymbol{u}^{\text{obs}}) + \frac{1}{2}\boldsymbol{u_0}^T\boldsymbol{\Gamma}_{\text{prior}}^{-1}\boldsymbol{u_0},$$

**The variational formulation of the elasticity BVP:**

$$\int_\Omega \boldsymbol{\varepsilon}(\boldsymbol{u}) : (\mathbb{C}\boldsymbol{\varepsilon}(\boldsymbol{v}))\,dx + \int_{\Gamma_b} \delta^{-1}(\boldsymbol{u}\cdot\boldsymbol{t}-\boldsymbol{u_0})\boldsymbol{v}\cdot\boldsymbol{t}\,dx = 0$$

The constitutive equation is: $\sigma(\mathrm{u}) = \mathbb{C}\,\epsilon(\mathrm{u})$, where $\mathbb{C}$ is the forth order linear elasticity tensor and $\epsilon(\mathrm{u})$ is the strain tensor. $\delta > 0$ is very small, therefore the Robin-type boundary condition can be understood as regularized Dirichlet condition.

We use the formal Lagrangian method to derive the gradient $\mathcal{G}$ of $\mathcal{J}$ with respect to $u_0$. This gradient vanishes at the minimum of $\mathcal{J}(\cdot)$, i.e., at the solution of the inverse problem.

**Lagrangian function:**

$$\mathcal{L}(\boldsymbol{u},\boldsymbol{u_0},\boldsymbol{v}) := \mathcal{J}(\boldsymbol{u_0},\boldsymbol{u}) + \int_\Omega \boldsymbol{\varepsilon}(\boldsymbol{u}) : \mathbb{C} : \boldsymbol{\varepsilon}(\boldsymbol{v})\,dx + \int_{\Gamma_b} \delta^{-1}(\boldsymbol{u}\cdot\boldsymbol{t}-\boldsymbol{u_0})\boldsymbol{v}\cdot\boldsymbol{t}\,dx \quad (1)$$

**Variations with respect to $\boldsymbol{u}$ and $\boldsymbol{u_0}$:**

$$\mathcal{L}_{\boldsymbol{u}}(\hat{\boldsymbol{u}}) = (\mathcal{B}\boldsymbol{u}-\boldsymbol{u}^{\text{obs}})^\top(\mathcal{B}\hat{\boldsymbol{u}}) + \int_\Omega \boldsymbol{\varepsilon}(\hat{\boldsymbol{u}}) : \mathbb{C} : \boldsymbol{\varepsilon}(\boldsymbol{v})\,dx + \int_{\Gamma_b} \delta^{-1}(\hat{\boldsymbol{u}}\cdot\boldsymbol{t})\boldsymbol{v}\cdot\boldsymbol{t}\,dx \quad (2)$$

$$\mathcal{L}_{u_0}(\hat{u}_0) = \boldsymbol{u_0}^T\boldsymbol{\Gamma}_{\text{prior}}^{-1}\hat{\boldsymbol{u}}_0 - \int_{\Gamma_b} \delta^{-1}\hat{\boldsymbol{u}}_0\boldsymbol{v}\cdot\boldsymbol{t}\,dx \quad (3)$$

## References

This material is based upon work supported by the National Science Foundation Graduate Research Fellowship under Grant No. DGE-1110007

DeShon, H. R., Schwartz, S. Y., Newman, A. V., Gonzalez, V., Protti, M., Dorman, L. M., Flueh, E. R. (2006). Seismogenic zone structure beneath the Nicoya Peninsula, Costa Rica, from three-dimensional local earthquake P - and S -wave tomography. Geophysical Journal International, 164(1), 109 -124.
Dixon, T.H. (1993). GPS measurement of relative plate motion of the Cocos and Caribbean plates and strain accumulation across the Middle America trench, 20(20), 2167-2170.
Feng, L., Newman, A. V., Protti, M., González-Ávalez, V., Jiang, Y., & Dixon, T. H. (2012). Active deformation near the Nicoya Peninsula, northwestern Costa Rica, between 1996 and 2010: Interseismic megathrust coupling. Journal of Geophysical Research, 117(B6)
Malservisi, R., S.Y. Schwartz, N. Voss, M. Protti, V. Gonzales, T.H. Dixon, Y. Jiang, A.V. Newman, J.A. Richardson, J.I. Walter, D. Voytenko (2015) Multiscale postseismic behavior on a megathrust: the 2012 Nicoya earthquake, Costa Rica, Geochem. Geophys. Geosyst., 16(6), 1848-1864, doi:10.1002/2015GC005794
Protti, M., Gonzalez, V., Newman, A. V., Dixon, T. H., Schwartz, S. Y., Marshall, J. S., Owen, S. E. (2013). Nicoya earthquake rupture anticipated by geodetic measurement of the locked plate interface. Nature Geoscience, 7(2), 117 - 121

## Inversion Results

**Right:** Solution for coseismic slip on the fault plane. The slip magnitude outlines the locked patch found previously and shows a maximum slip of 2.5 meters under the Nicoya peninsula. Slip vectors are represented by the blue arrows. Contour lines show depth of the slab. The magnitude of the modeled slip patch is 7.66 $M_w$. The magnitude was used to choose an appropriate correlation length between points.

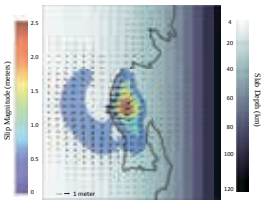


**Below:** surface displacement vectors. Blue arrows represent the displacements taken from GPS stations (data). Red arrows are the solution to the inverse model at the GPS station locations. The model attempts to minimize the difference between the two while enforcing smoothness in the solution.

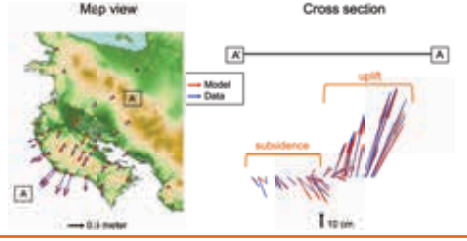


## Poroelasticity in Subduction Zones

**Relationship between pore fluid and the seismic cycle**

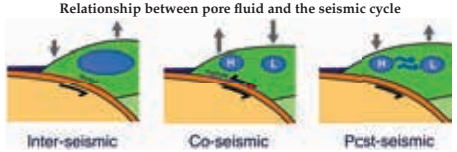


$$(S_\epsilon p + \alpha\nabla\cdot u)_t - \nabla\cdot(\kappa/\mu\nabla p) = 0$$
$$-\nabla\cdot(\boldsymbol{\sigma}(u) - \alpha p\boldsymbol{I}) = 0$$

where $\boldsymbol{p}$ is pore pressure and $\boldsymbol{u}$ is rock displacement

## Post-seismic Deformation Response

**Right:** Pressure response at 1 km depth. A groudwater well located at 10°3.800'N, 85°15.633'W that overflowed for minutes after the earthquake falls within the high pressure region. The initial earthquake-induced pressure largely dissipates after 3 months.

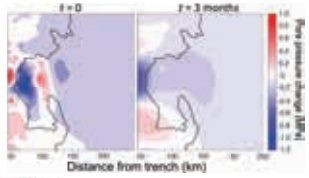


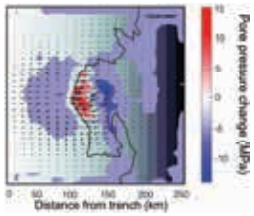


**Left:** Induced pore pressure change above the subducting slab. The pressure change is an order of magnitude larger than near the surface. Additionally, the locked patch produces a second area of pressure drop offshore. In the absence of secondary permeability, the induced pressure change persists for months (at least) after the earthquake.

**Right:** Modeled time series of post-seismic surface deformation. Due solely to fluid flow, there is a 10 day rebound of the surface after the earthquake an areas of extreme high and low pore pressure. In intermediate areas, the modeled response is more complex and often non-monotonic.

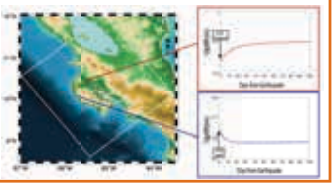

## Discussion and Future Work

- **Poroelastic relaxation is likely a significant contributor to the post-seismic deformation signal.**
- **With the contraint of well data, we can begin to parse out the poroelastic response from afterslip and viscoelastic signals.**
- **Next steps: Examine the posterior pdfs, calculate uncertainties and test boundary conditions.**
- **Can aftershocks tell us anything about fluid migration after a megathrust earthquake?**
- **A giant pump test: Can we use post-seismic fluid flow to constrain regional permeability?**

# Numerical modeling of initial slip and poroelastic effects of the 2012 Costa Rica earthquake

McCormack, Kimberly A.[1]*, Hesse, M. A.[1], Stadler, G.[2]
1.Department of Geosciences, The University of Texas at Austin *kimberly.mccormack@utexas.edu
2.Courant Institute of Mathematical Sciences, New York University

## Background

On September 5th, 2012 a major megathrust earthquake ($M_w$=7.6) ruptured the plate interface beneath the Nicoya Peninsula, Costa Rica. The epicenter was located 12km offshore of the central Nicoya coast, at a depth of 18km. The rupture spread outward along the plate interface to encompass 3000 km$^2$ of the Nicoya seismogenic zone. More than 1,700 aftershocks were recorded within the first five days. With the exception of the imaged 'locked patch', the plate ruptured within a zone that previously deteremined to be seismically coupled.

The Nicoya Pennisula, uniquely positioned over the seismogenic zone the the subduction zone, allows more direct observations of fault slip via land-based GPS measurements. During the earthquake a total of 37 stations (both continuous and campaign) were deployed.

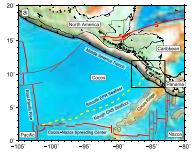


(Feng, 2012)

## Motivation

- **Is poroelastic relaxation a significant part of post-seismic deformation patterns?**
- **Can we differentiate it from afterslip and viscoelasticity?**
- **How is stress transferred by post-seismic fluid flow?**

## GPS Data / Model Outline

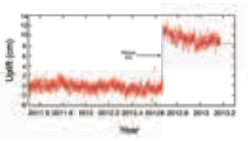

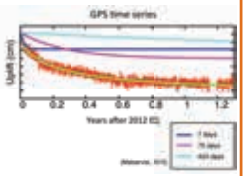


**Model Outline**

Surface displacement from GPS stations

Solve Inverse Problem

Instantaneous displacement on fault

Solve Forward Problem

Rock displacement and pore pressure evolution

We formulate a Bayesian inverse problem to infer the co-seismic slip on the fault plane based on instantaneous surface displacements taken from high-rate GPS stations (**top left**). The solution to the inversion is then taken as the initial condition to the time-dependent forward problem which models how both pore pressure and rock displacement evolve after the earthquake.

## Model Geometry

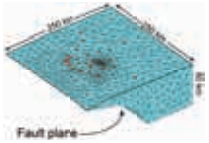


3D finite element model geometry (above). Red circles represent the locations of GPS stations.

**Elasticity Boundary Value Problem:**

$$\begin{aligned} -\nabla \cdot \boldsymbol{\sigma}(\mathbf{u}) &= 0 \quad \text{in } \Omega \\ \boldsymbol{\sigma}(\boldsymbol{u})\boldsymbol{n} &= 0 \quad \text{on } \Gamma_{top} \\ \boldsymbol{u} &= 0 \quad \text{on } \Gamma_{side} \\ \boldsymbol{u} \cdot \boldsymbol{n} &= 0 \quad \text{on } \Gamma_{bottom} \\ (\boldsymbol{I} - \boldsymbol{n}\boldsymbol{n}^\top)\boldsymbol{u} &= \boldsymbol{u_0} \quad \text{on } \Gamma_{bottom} \end{aligned}$$

## Inversion for slip distribution

To formulate the inverse problem, we assume a vector of surface observations $\boldsymbol{u}^{\text{obs}}$ and a corresponding surface observation operator $\mathcal{B}$, which evaluates the displacement at points on the top surface $\Gamma_{top}$. Then, the inverse problem with a regularization based on the distance between observation points for the unknown displacement $\boldsymbol{u_0}$ on $\Gamma_{bottom}$ is:

**Cost functional:**

$$\mathcal{J}(\boldsymbol{u_0}, \boldsymbol{u}) = \min_{\boldsymbol{u_0} \in L^2(\Gamma_b)} \mathcal{J}(\boldsymbol{u_0}) := \frac{1}{2}(\mathcal{B}\boldsymbol{u} - \boldsymbol{u}^{\text{obs}})^\top \boldsymbol{\Gamma}_{\text{noise}}^{-1}(\mathcal{B}\boldsymbol{u}_d - \boldsymbol{u}^{\text{obs}}) + \frac{1}{2}\boldsymbol{u_0}^T \boldsymbol{\Gamma}_{\text{prior}}^{-1}\boldsymbol{u_0},$$

**The variational formulation of the elasticity BVP:**

$$\int_\Omega \boldsymbol{\varepsilon}(\boldsymbol{u}) : (\mathbb{C}\boldsymbol{\varepsilon}(\boldsymbol{v}))\, dx + \int_{\Gamma_b} \delta^{-1}(\boldsymbol{u} \cdot \boldsymbol{t} - \boldsymbol{u_0})\boldsymbol{v} \cdot \boldsymbol{t}\, dx = 0$$

The constitutive equation is: $\sigma(\mathrm{u}) = \mathbb{C}\, \epsilon(\mathrm{u})$, where $\mathbb{C}$ is the forth order linear elasticity tensor and $\epsilon(\mathrm{u})$ is the strain tensor. $\delta > 0$ is very small, therefore the Robin-type boundary condition can be understood as regularized Dirichlet condition.

We use the formal Lagrangian method to derive the gradient $\mathcal{G}$ of $\mathcal{J}$ with respect to $u_0$. This gradient vanishes at the minimum of $\mathcal{J}(\cdot)$, i.e., at the solution of the inverse problem.

**Lagrangian function:**

$$\mathcal{L}(\boldsymbol{u}, \boldsymbol{u_0}, \boldsymbol{v}) := \tilde{\mathcal{J}}(\boldsymbol{u_0}, \boldsymbol{u}) + \int_\Omega \boldsymbol{\varepsilon}(\boldsymbol{u}) : \mathbb{C} : \boldsymbol{\varepsilon}(\boldsymbol{v})\, dx + \int_{\Gamma_b} \delta^{-1}(\boldsymbol{u} \cdot \boldsymbol{t} - \boldsymbol{u_0})\boldsymbol{v} \cdot \boldsymbol{t}\, dx \quad (1)$$

**Variations with respect to $\boldsymbol{u}$ and $\boldsymbol{u_0}$:**

$$\mathcal{L}_{\boldsymbol{u}}(\hat{\boldsymbol{u}}) = (\mathcal{B}\boldsymbol{u} - \boldsymbol{u}^{\text{obs}})^\top (\mathcal{B}\hat{\boldsymbol{u}}) + \int_\Omega \boldsymbol{\varepsilon}(\hat{\boldsymbol{u}}) : \mathbb{C} : \boldsymbol{\varepsilon}(\boldsymbol{v})\, dx + \int_{\Gamma_b} \delta^{-1}(\hat{\boldsymbol{u}} \cdot \boldsymbol{t})\boldsymbol{v} \cdot \boldsymbol{t}\, dx \quad (2)$$

$$\mathcal{L}_{u_0}(\hat{u}_0) = \boldsymbol{u_0}^T \boldsymbol{\Gamma}_{\text{prior}}^{-1}\hat{\boldsymbol{u}}_0 - \int_{\Gamma_b} \delta^{-1}\hat{\boldsymbol{u}}_0 \boldsymbol{v} \cdot \boldsymbol{t}\, dx \quad (3)$$

## References

This material is based upon work supported by the National Science Foundation Graduate Research Fellowship under Grant No. DGE-1110007

DeShon, H. R., Schwartz, S. Y., Newman, A. V., Gonzalez, V., Protti, M., Dorman, L. M., Flueh, E. R. (2006). Seismogenic zone structure beneath the Nicoya Peninsula, Costa Rica, from three-dimensional local earthquake P - and S -wave tomography. Geophysical Journal International, 164(1), 109 -124.
Dixon, T.H. (1993). GPS measurement of relative plate motion of the Cocos and Caribbean plates and strain accumulation across the Middle America trench, 20(20), 2167-2170.
Feng, L., Newman, A. V., Protti, M., González-Ávalez, V., Jiang, Y., & Dixon, T. H. (2012). Active deformation near the Nicoya Peninsula, northwestern Costa Rica, between 1996 and 2010: Interseismic megathrust coupling. Journal of Geophysical Research, 117(B6)
Malservisi, R., S.Y. Schwartz, N. Voss, M. Protti, V. Gonzales, T.H. Dixon, Y. Jiang, A.V. Newman, J.A. Richardson, J.I. Walter, D. Voytenko (2015) Multiscale postseismic behavior on a megathrust: the 2012 Nicoya earthquake, Costa Rica, Geochem. Geophys. Geosyst., 16(6), 1848-1864, doi:10.1002/2015GC005794
Protti, M., Gonzalez, V., Newman, A. V., Dixon, T. H., Schwartz, S. Y., Marshall, J. S., Owen, S. E. (2013). Nicoya earthquake rupture anticipated by geodetic measurement of the locked plate interface. Nature Geoscience, 7(2), 117 - 121

## Inversion Results

**Right:** Solution for coseismic slip on the fault plane. The slip magnitude outlines the locked patch found previously and shows a maximum slip of 2.5 meters under the Nicoya peninsula. Slip vectors are represented by the blue arrows. Contour lines show depth of the slab. The magnitude of the modeled slip patch is 7.66 $M_w$. The magnitude was used to choose an appropriate correlation length between points.

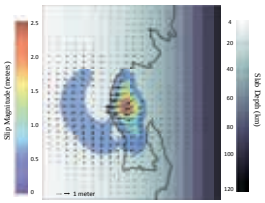


**Below:** surface displacement vectors. Blue arrows represent the displacements taken from GPS stations (data). Red arrows are the solution to the inverse model at the GPS station locations. The model attempts to minimize the difference between the two while enforcing smoothness in the solution.

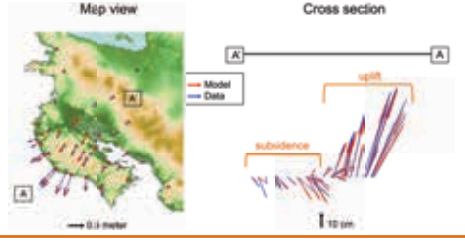


## Poroelasticity in Subduction Zones

**Relationship between pore fluid and the seismic cycle**

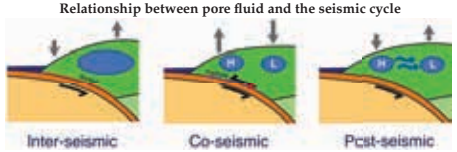


$$\begin{aligned} (S_\epsilon p + \alpha \nabla \cdot u)_t - \nabla \cdot (\kappa/\mu \nabla p) &= 0 \\ -\nabla \cdot (\boldsymbol{\sigma}(u) - \alpha p \boldsymbol{I}) &= 0 \end{aligned}$$

where $\boldsymbol{p}$ is pore pressure and $\boldsymbol{u}$ is rock displacement

## Post-seismic Deformation Response

**Right:** Pressure response at 1 km depth. A groudwater well located at 10°3.800'N, 85°15.633'W that overflowed for minutes after the earthquake falls within the high pressure region. The initial earthquake-induced pressure largely dissipates after 3 months.

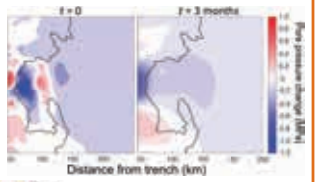


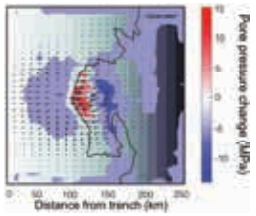


**Left:** Induced pore pressure change above the subducting slab. The pressure change is an order of magnitude larger than near the surface. Additionally, the locked patch produces a second area of pressure drop offshore. In the absence of secondary permeability, the induced pressure change persists for months (at least) after the earthquake.

**Right:** Modeled time series of post-seismic surface deformation. Due solely to fluid flow, there is a 10 day rebound of the surface after the earthquake an areas of extreme high and low pore pressure. In intermediate areas, the modeled response is more complex and often non-monotonic.

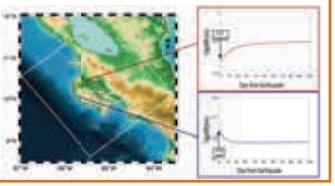

## Discussion and Future Work

- **Poroelastic relaxation is likely a significant contributor to the post-seismic deformation signal.**
- **With the contraint of well data, we can begin to parse out the poroelastic response from afterslip and viscoelastic signals.**
- **Next steps: Examine the posterior pdfs, calculate uncertainties and test boundary conditions.**
- **Can aftershocks tell us anything about fluid migration after a megathrust earthquake?**
- **A giant pump test: Can we use post-seismic fluid flow to constrain regional permeability?**